

Photo Catalysis Desulfurization at Copper Oxides /Titanium Oxide Nanotubes Under UV and Visible Light Irradiation

Hameed Hussein Alwan*

Chemical Engineering Department, College of Engineering, University of Babylon, Iraq

Received 19 May 2021; received in revised form 6 October 2021; accepted 25 October 2021

ABSTRACT

Titanium dioxide nanotubes TNTs were synthesized by anodization in a fluoride-based electrolyte, TNTs are commonly working as photocatalytic under ultraviolet UV irradiation via its wide bandgap, and it was expanded under visible light irradiation by doping with other metals or metals oxides, herein TNTs were doped by copper oxides Cu_2O and CuO to produce copper oxides /titanium oxide nanotubes CuOx/TNT . The prepared catalysts (TNTs and CuOx/TNT) were characterized by XRD, FTIR, SEM and, EDX, while catalysts activity was investigated for oxidization of Dibenzothiophene DBT under ultraviolet UV and visible light VL irradiations, the feedstock is model fuel (heptane contains DBT as a sulfur component) was oxidized by hydrogen peroxide H_2O_2 . Results showed that TNT has a moderate catalysis effect under UV irradiation and a low catalysis effect under VL irradiation. CuOx/TNT catalyst exhibited good sensitivity for VL radiation. The study investigated the effect of initial DBT concentration, oxidant dosage, reaction temperature, contact time, and type of irradiation on oxidation desulfurization ODS reaction by using TNT and CuOx/TNT catalysts, the results showed that DBT removal efficiency was increasing with temperature (56.2, 80.4 and 91.2 at 40,50, and 60 °C respectively at 100 minutes) and oxidant amount (66.4, 80.4, and 86.1 by adding 5,10,15 ml of oxidant respectively at 100 minutes) while it decreases with the increasing initial BDT concentration (94.8, 80.4, and 86.1 when using 100,150, and 200 ppm as initial DBT concentration at 100 minutes). The kinetics calculations exhibited that ODS reaction under VL irradiation follows pseudo-first-order reaction at CuOx/TNT catalyst with reaction rate constants of 0.00076, 0.0108 and 0.0141 min^{-1} at 40,50, and 60°C respectively, the activation energy for the reaction is 26.8 kJ/mol, negative ΔS (-0.218 kJ/mol.K) and positive ΔH and ΔG for DBT oxidation under UV irradiation.

Keywords: TiO_2 Nanotubes, Photo catalyst, Catalysis, Reaction kinetics, Desulfurization, Dibenzothiophene.

1. Introduction

Titanium oxide TiO_2 is one of the most important materials which present mainly three crystalline phases; anatase, rutile, and brookite, and has many promising properties that make it a good candidate it for many application e.g. photocatalysis, dye-sensitized cells, biomedical devices, gas sensing, pollutant degradation, etc., anatase and rutile showed optical band gaps of 3.2 and 3.0 eV respectively while TiO_2 nanotubes TNT amorphous and anatase showed the bandgap of 3.2 eV, Zwilling et al. in 1999 reported the feasibility of growing TiO_2 nanotubes TNT arrays by titanium electrochemical anodization. The specific ionic and electronic properties for TiO_2 depended on the crystalli-

-ne phase in which anatase phase exhibited the highest electron mobility so it is the most desirable crystalline structure prefer for electron-conduction applications like photocatalysis and solar cell applications [1-2].

As mentioned above TiO_2 has a wide bandgap and this leads to quick recombination for photo-generated electron-hole especially under VL radiation which restricted its use for some specific applications. Despite the wide bandgap of TiO_2 , it can absorb 5% of sun radiation including VL. To overcome that, it was suggested to implant it with the number of different ions (anions or cations) by doping with metallic or nonmetallic elements to extend its work for VL regions and enhance separation of electron-hole, several methods have been proposed for expanding the range of TiO_2 to absorb VL; one of these methods is doping TiO_2

*Corresponding author:

E-mail address: hameed@uobabylon.edu.iq (H. H. Alwan)

lattice with some materials. This approach is adding semiconductor materials with a narrow bandgap for charge carrier lifetime increasing from delayed recombination reaction [3-5].

Considering physical stability and matching type of interface to facilities the transport of carrier, copper oxides p-Type semiconductor is an exquisite material. Copper oxides have two well-known forms; CuO (cuprite) and Cu₂O (tenorite), CuO is characterized by selective solar absorption via its low thermal emitting and high solar absorption. Cu₂O and CuO are semiconductors having an energy bandgap of about 1.21-1.5 eV and 2.0-2.5 eV respectively which depend on the method of preparation and conditions. Copper oxides have the capability of performing under sunlight irradiation because the presence of Cu⁺/Cu⁺² causes oxidative transformation of organic compounds. Copper oxide gives the highest degradation rate compared to other metal oxides; it was found that catalyst activity increases with CuO loading increasing as well as high CuO dispersion [6-9].

Removing or minimizing sulfur from the fuel is a big challenge for scientist and researchers because sulfur present in this fuel lead has harmful effects on human health and environment via acid rains formation from sulfur oxides emissions after these fuels are burned as well as it causes corrosion in upstream refineries equipment and catalyst poisoning at catalyst reforming unit. Many techniques were used for removing or minimize sulfur content. Hydrodesulphurization (HDS) process is a conventional method used for removing or minimizing sulfur content, but it is necessary to provide an active catalysts, elevated temperatures and pressures as well as a huge amount of hydrogen gas. HDS method is not effective in removing some sulfur compounds from petroleum products such as heterocyclic organic compounds; Dibenzothiophene (DBT) and Benzothiophenes (BT). Many techniques can be used as an alternative to HDS; one of these methods is Oxidation desulfurization (ODS) which is considered as a promising process for high sulfur removing even at moderate operation conditions e.g. ambient temperature and atmospheric pressure. Many oxidative agents are applied in ODS processes such as hydrogen peroxide H₂O₂ and ozone O₃ [10-11].

Hydrogen peroxide is used as a green oxidant in the advanced oxidation process i.e. UV/H₂O₂ catalysis process. Like some components founded in the peroxide group, H₂O₂ consists of a weak O-O bond, which is susceptible to heat and light. For H₂O₂ activation for reactive oxidizing radical production, a catalyst was required, and TiO₂ had been investigated as a potential

catalyst which is able to generate a strong oxidizing media [12]. Many researchers focused on H₂O₂ decomposition on TiO₂ surface dispersed in an aqueous solution under UV irradiation, and they proposed a mechanism which mainly focused on trying for enhancing organic pollutants removal efficiency in the presence of hydrogen peroxide by eliminating recombination between conduction band CB electron and valance band VB hole [13].

Heterogeneous photocatalytic degradation of pollutants in wastewater has been described as an effective technique to solve environmental problems caused by pollutants, in which heterogeneous photocatalysis fundamentals are based on catalysts prepared by the combination of semiconductors e.g. metal oxides with metal sulfides in UV irradiation. Semiconductors adsorb light energy same as or greater than their bandgap energy, the excited electron, and generated holes are responsible in free radicals generation leading to the oxidation and production of the organic stray [14].

This study was conducted to enhance photocatalysis activity for TNT under VL irradiation, and TNT was synthesized by electrochemical anodization and doping with copper oxides by electrodepositing, the photocatalytic activity was examined by DBT oxidation with H₂O₂ at different reaction parameters; time, temperature, initial BDT concentration and oxidant amount.

2. Experimental

2.1. Materials

Titanium Ti foils (purity 99% with 0.1 mm thickness) were provided. Dibenzothiophene DBT, heptane, acetonitrile, acetone, ammonium fluoride, ethylene glycol, lactic acid, and ethanol were of analytical grade.. The deionized water DW used in work was produced in the lab.

2.2. Synthesis of TNT

Ti foil was cut to a slip with dimensions (1 cm × 1 cm) and washed with acetone, and ethanol separately for 10 minutes each under sonication, and then rinsed with deionized water DW and dried by air. TNTs is synthesized by electrochemical at specified anodization conditions, based on literature, self-organized TNT was developed at various media, here ethylene glycol-based electrolyte; 0.37 grams of NH₄F, and 1.8 mL of DW were added to 100 mL of ethylene glycol to produce 0.1 M of NH₄F and 0.1 M H₂O solutions. The pretreated Ti foil was immersed in the electrolyte and acted as an anode while the platinum electrode is used as the cathode; the distance between two electrodes was kept

constant (2 cm) while the power supply was switched on for 10, 20, 30, and 60 minutes at 10 volts. The TNT formed after anodization was cleaned with ethanol and dried by air, then washed with DW and subsequently calcinated at 450 °C for 1 hour.

2.3. CuO and Cu₂O electrodeposition on TNT

The prepared TNT acted as a cathode, while the Pt electrode acted as an anode, both electrodes were immersed in electrolyte consisting of 0.4 M copper nitrate solution Cu(NO₃)₂.6H₂O and Lactic acid for 40 seconds at a current density of 10 mA/cm² at room temperature and pH = 5 [15]; after electrodeposition step the CuOx/TNT was cleaned with ethanol and rinsed with DW followed by calcination at 450 °C for 1 hour.

2.4. Catalyst characterization

X-ray diffraction XRD type (Shimadzu model 6000), Fourier Transform Infrared Spectroscopy FTIR and, Energy Dispersion Spectrometry EDS (BRUKER Model X Flash 6110 Germany) were used to characterize the prepared TNT and CuOx/TNT, while the surface morphology was investigated by scanning electronic spectroscopy SEM (HITACHI SEM FE S4800).

2.5. Photo catalytic experiments

A photocatalytic ODS reaction was used to remove sulfur from model fuel (heptane contained DBT), the oxidant agent used is 30 wt. % H₂O₂. Batch reactor was irradiated by VL (provided 350 W lamp type HP mercury) or by UV (provided by 2 UV lamps × 15 watts), the light source was put at a distance of 10 cm from the reactor. The reaction system is a glass flask (its size 50 mL) that was put in a water bath to maintain temperature at a defined value. The prepared catalysts (TNT or CuOx/TNT) were immersed in the glass flask containing 30 ml of model fuel with continues stirring; model fuel contains the initial concentration of sulfur (S₀), the reactor with its content was placed in dark for about 45 minutes to reach equilibrium state [16].

The H₂O₂ was added to the reactor and was exposed to light at the same time, the reaction stopped after a specific time to start another experiment for different operation conditions. The collected sample was divided into two layers, this will be separated by adding acetonitrile, and the upper layer is taken for analysis to measure the final sulfur concentration (S_f). Total sulfur content was measured using the sulfur meter (type RX-620SA/TANKA SCIENTIFIC), to calculate DBT removal efficiency, RE% was calculated as follows:

$$RE\% = \frac{S_0 - S_f}{S_0} \times 100 \quad (1)$$

Where, S₀ is initial total sulfur content, S_f is final total sulfur content.

3. Results and Discussion

3.1. Characterizations

Fig. 1 shows the top and side views as TNT prepared at different anodization times, as seen in this figure, the thick layer of TNT increases with increasing anodization time, and this is in agreement with much previous work [17-18], the nanotube layer thickness is 5.46, 9.58, 14.07 and 24.61 μm at 10, 20, 30, and 60 minutes respectively, the diameter of the nanotube approximates to 39, 55, 66, and 105 nm at 10, 20, 30, and 60 minutes respectively. **Fig. 2** shows the layer as a function of anodization time; the layer thickness is proportional to increasing anodization time [18]. In this study, the TNT with a high thickness (24.61 μm) was chosen for photocatalytic because the high activity can be achieved with long tubes as the reaction rate increased with thickness [19].

XRD patterns for prepared TNT before calcination was shown in **Fig. 3**, it was seen that formed TNT is comprised of amorphous TiO₂ as shown in curve (a) in **Fig. 3**. TNT after calcination at 450 °C, as seen in curve (b); various stages of crystallization were shown in this figure. Formation of anatase TiO₂ phase was accelerated at formation above 280 °C while formation of rutile TiO₂ phase increases at above 500 °C [2]. The curve (b) in **Fig. 3** has peaks at 2θ = 25.4, 37.6, 48.1, and 62.3 ° which refer to anatase TiO₂ (A-TiO₂) and 2θ = 27.5 corresponds to the rutile phase (R-TiO₂) [19-21], the antasa phase has more chance to appear because the calcination step is done at 450°C as reported in many previous works of literature [2]. Curve (c) shows the XRD pattern of CuOx /TNT catalyst as seen apart from anatase and rutile TiO₂ mentioned above, there are many peaks at 2θ=36.4, 45.2 and 57.9 which are corresponding to CuO [22], and 2θ = 61.1 is corresponding to Cu₂O [23]. The CuO crystal size d_P for as prepared CuOx /TNT samples was determined by calculating the most intense peak broad according to the Debye-Scherrer equation

$$d_P = \frac{\kappa\lambda}{\beta \cos\theta} \quad (2)$$

Where κ is the correction factor which accounts for the particle shape (and it equal 0.94), β is full width at half maximum FWHM while λ is the wavelength of Cu target (0.1518 Å) and θ is Bragg's angle [21], [22-24].

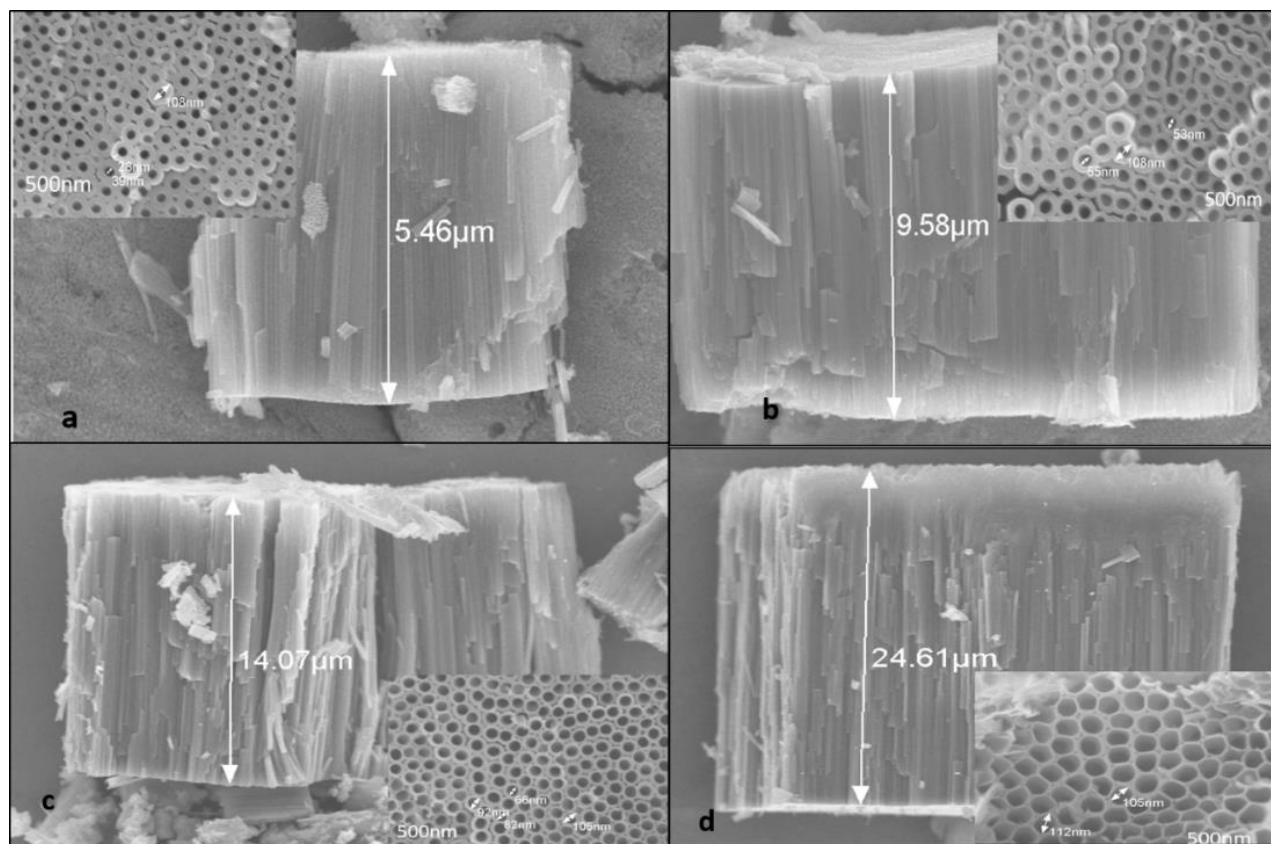


Fig. 1: SEM image for TNT produced at different anodization time (a) 10 minutes, (b) 20 minutes, (c) 30 minutes, and (d) 60 minutes.

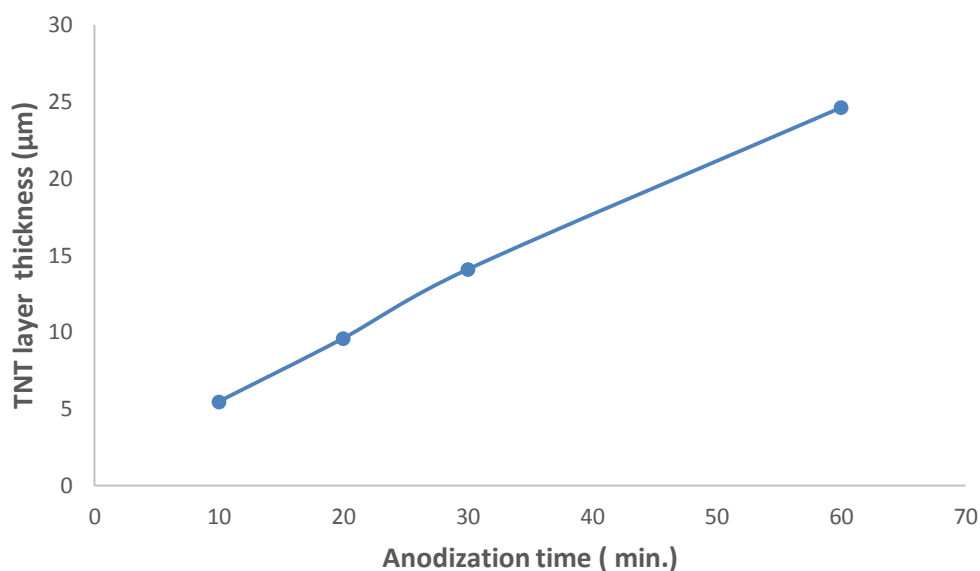


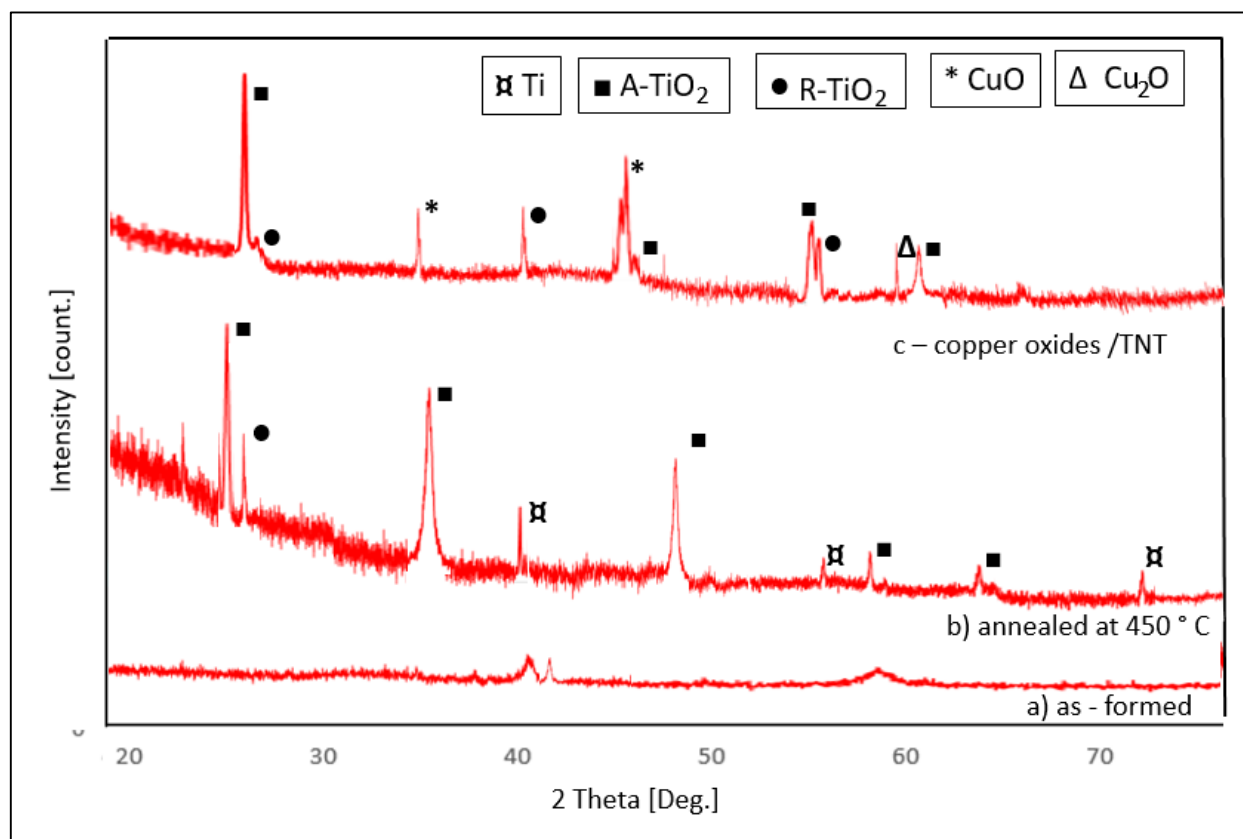
Fig.2. Effect of anodization time on developed TNT thickness layer.

From **Fig. 3**, the most intense peaks for CuO at 2θ is equal to 36.48 and 45.2°, while for Cu₂O, it is equal to 61.1°. Now by applying the Debye-Scherrer equation, the crystal size for CuO is 71, 27, and 68 nm, the crystal size for Cu₂O is 81 nm as listed in **Table 1**.

The elements mapping for CuOx /TNT was shown in EDX analyses at **Fig. 4**, which refer to the presence of copper and titanium as well as oxygen.

Table 1; the structural parameters of A-TiO₂, R-TiO₂, CuO and Cu₂O phases

2θ(°)	(hkl)	FWHM(β) (°)	d-spacing (Å)	Crystal size (d _p) (nm)
25.41	(120)	0.287	4.1764	50
27.56	(101)	0.363	2.596	112
36.48	(100)	0.244	2.3976	71
37.65	(201)	0.308	2.2807	46
45.21	(004)	0.137	2.0982	27
48.23	(211)	0.268	1.7595	101
57.91	(112)	0.272	1.7567	68
61.15	(101)	0.264	1.4935	81
62.34	(132)	0.193	1.3572	76

**Fig.3:** XRD pattern for (a) as formed TNT, (b) TNT after annealed at 450 °C and (c) for CuOx/TNT.

The prepared catalyst CuOx/TNT was shown at SEM images in **Fig. 5**, the copper oxides particles were observed obviously at the top of TiO₂ nanotubes and this means that the copper oxides were deposited in electrodeposition steps; on the other hand, the TNT arrays were disordered in comparison with TNT array before copper electrodeposition, and this disorder is due to hypothesized as a result of mechanical stress at Cu/Ti phase boundary, Q. Ma reported that disordering obviously for longer TNT near the boundary [25].

3.2. Effect of studied variables on desulfurization oxidation reaction

3.2.1. Effect of catalyst and type of light irradiation

To investigate the effect of radiation types on photocatalysis activity of TNT catalyst for DBT removal efficiency from model fuel, it was radiated by UV light and visible light VL, the results showed that DBT removal efficiency under UV irradiation is higher than that under VL irradiation as indicated in **Fig. 6** because TiO₂ has a wide-band gap: 3.2 eV and 3 eV for

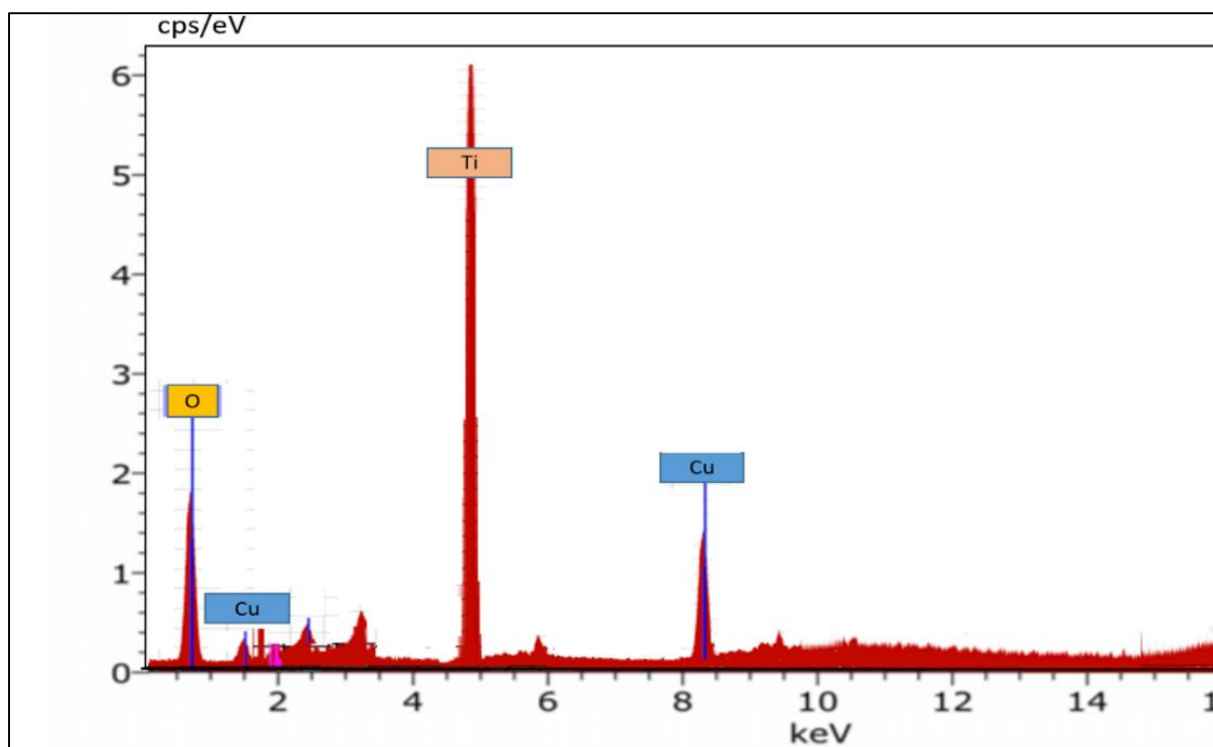


Fig. 4: EDX analyses shows the elements mapping for CuOx/TNT.

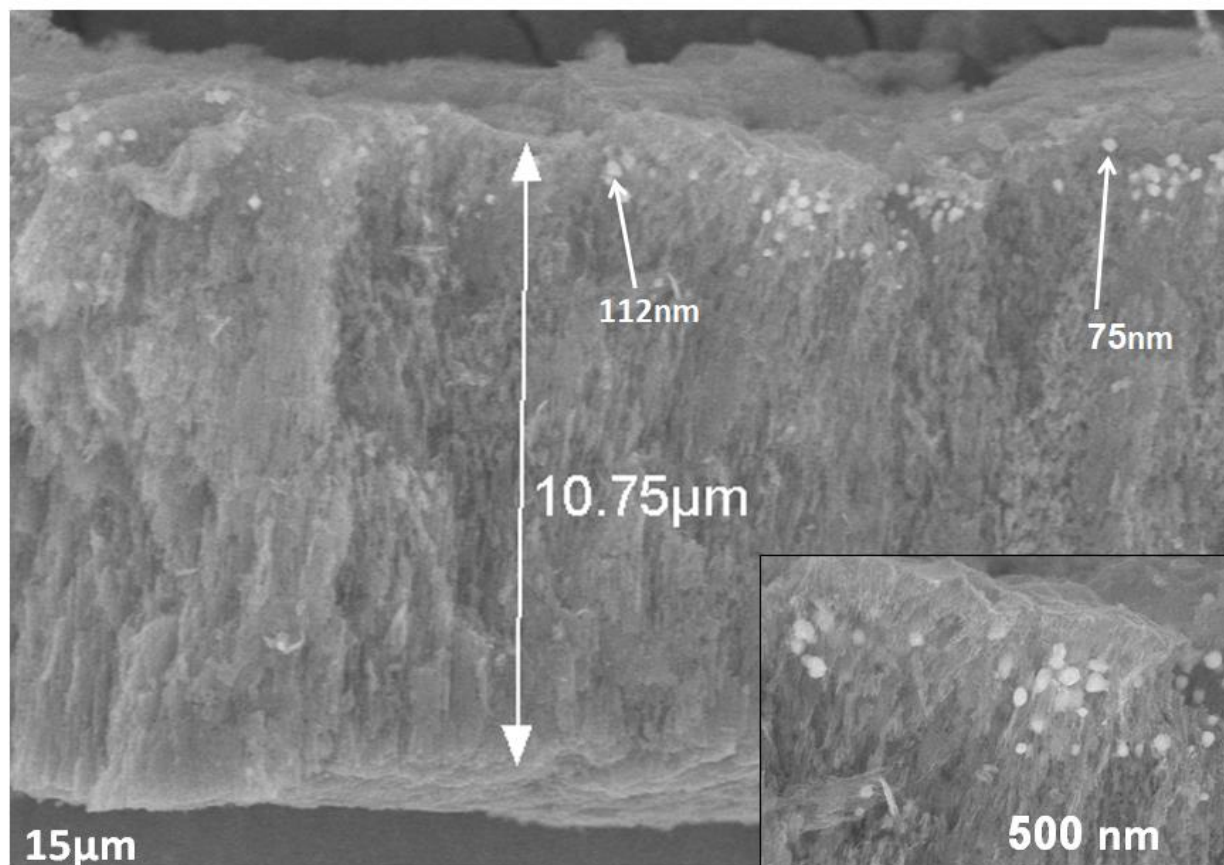


Fig.5: SEM image for CuOx/TNT catalyst, showing CuO and Cu₂O particles diameter about 75-112 nm.

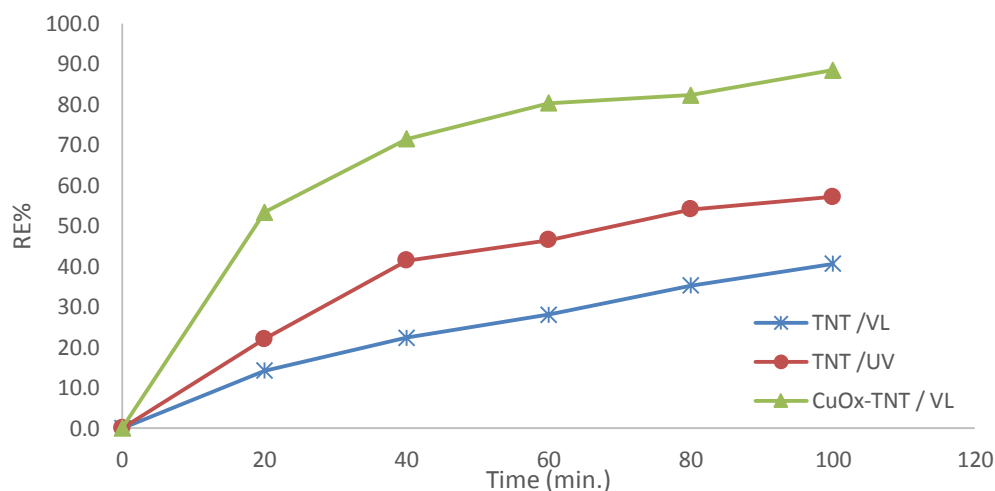


Fig.6: effect of using different catalyst on DBT removal efficiency, at 50 °C, and using initial DBT concentration 150 mg/L in pentane under irradiation time for 100 minutes and 10 mL H₂O₂ as oxidant agent under irradiation of visible and UV light.

anatase and rutile phase respectively and this makes it excited under UV light with wavelength not longer than 387.5 nm, thus TiO₂ is approximately inactive under visible light which makes it useful not more than 5% from sunlight (VL) [26]. The enhancement of TNT layer photocatalytic under VL irradiation was done by doped TNT also shown in Fig. 7, by using CuOx/TNT catalyst the results showed good DBT removal efficiency from model fuel and this is due to adding copper oxides to TNT layer, it was well known that copper oxides are characterized by its narrow bandgap; 1.21-1.5 and 2.0-2.5 eV for CuO and Cu₂O respectively. The excited electron transfers from TiO₂ valence band to TiO₂ conduction energy level to copper oxides conduction band thus photocatalytic activity was enhanced via the charge recombination suppressed on TiO₂ and oxidation promotion on TiO₂ by holes and reduction at copper oxide by electron transfer [27].

3.2.2. Effect of reaction temperature on DBT removal efficiency

The temperature is described as the most important variable on chemical reaction and it was noted that reaction rate was proportional directly to the increasing reaction temperature. Fig. 7 shows the effect of temperature on DBT removal efficiency from model fuel, in which the DBT oxidation was increasing with temperature, the maximum DBT removal efficiency by using CuOx/TiO₂ catalyst are 56.2, 88.5 and 91.2 at 40, 50, and 60 °C respectively under VL irradiation for 100 minutes; therefore, the increase of temperature leads to the acceleration of reaction rate due to increasing of internal motion of molecules, thus DBT removal efficiency was enhanced by increasing temperature of the reaction [10-11] and , [28-30].

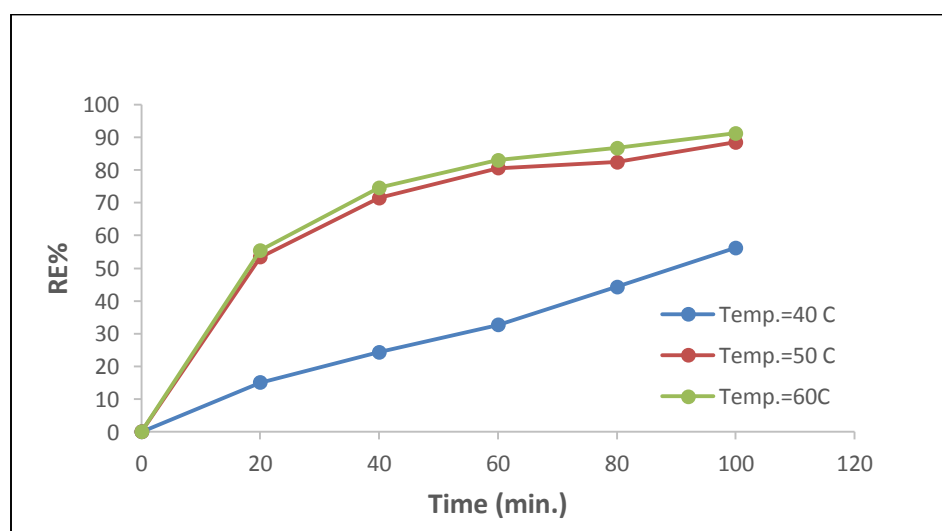


Fig.7: effect temperature on DBT removal efficiency, by of using CuOx /TNT as catalyst and using initial DBT concentration 150 mg/L in pentane, 10 ml H₂O₂ as oxidant agent under irradiation of visible light.

3.2.3. Effect of initial DBT concentration on DBT removal efficiency

DBT removal efficiency from model fuel was decreased with increasing the initial DBT (sulfur content) concentration as shown in Fig. 8, the maximum DBT removal efficiency was 94.8, 88.5, and 68.1 when the initial DBT concentration is 100, 150, and 200 mg/L in pentane used after 100 minutes, and at 50° C with using constant oxidant amount (10 ml). Based on these result, CuOx/TNT, the initial DBT concentration is an important parameter which limit catalyst application range [31].

3.2.4. Effect of oxidant amount on DBT removal efficiency

Different amounts of H₂O₂ was used (5, 10, 15 ml) with constant model fuel volume (30 ml) and constant initial DBT concentration (150 mg/L), at 50 °C; the reaction was conducted using CuOx/TNT catalyst under VL irradiation, as seen in Fig. 9 the DBT removal efficiency was increasing with an increasing amount of oxidant (66.4, 80.4, and 93.1 with using 5, 10, 15 ml of oxidant respectively) this is because DBT oxidation was enhanced by increasing of oxygen active radicals which caused DBT oxidation promotion, As seen in Fig. 10, the comparison of increasing of DBT removal efficiency between case after adding 5 and 10 ml is more than that after adding 10 and 15 ml of oxidant and this is via poisoning of the catalyst due to adding H₂O₂ as well as this increasing of H₂O₂ will increasing water in system which caused decreasing of oxidation rate [15], [32].

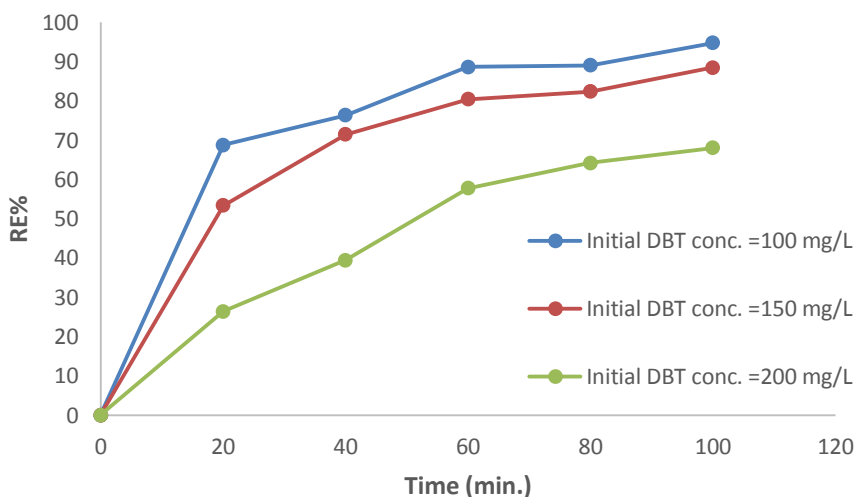


Fig.8: effect initial DBT concentration on DBT removal efficiency, by of using CuOx/TNT as catalyst and using 10 ml H₂O₂ as oxidant agent at 50° C under irradiation of visible light.

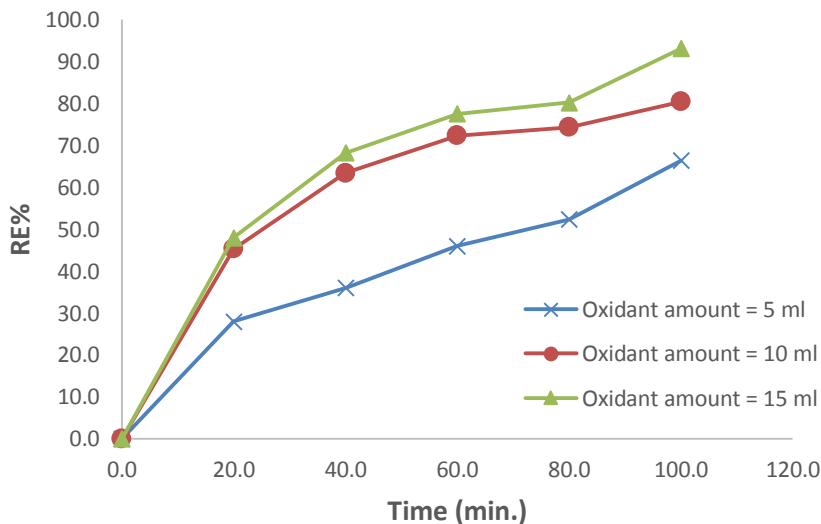
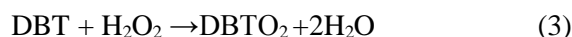


Fig.9: effect oxidant amount on DBT removal efficiency, by of using CuOx/TNT as catalyst and using initial DBT concentration 150 mg/L in pentane, at 50 °C as oxidant agent under irradiation of visible light.

3.2.5. DBT oxidation reaction kinetics and thermodynamics

To estimate kinetics parameters (reaction order, rate of reaction constants and activation energy) for DBT oxidation reaction, the kinetics were studied and the DBT oxidation results at different temperatures were considered, for the following reaction:



$$r = -\frac{d[\text{C}_{\text{DBT}}]}{dt} = k[\text{C}_{\text{H}_2\text{O}_2}]^m [\text{C}_{\text{DBT}}]^n \quad (4)$$

Where r is reaction rate, k is the apparent reaction rate constant and C_{DBT} is concentration of DBT, n is reaction order in respect to DBT concentration and m is reaction order with respect to H_2O_2 concentration. Many previous works reported that aromatic sulfur materials oxidation at solid catalyst follows pseudo 1st order reaction, and this happens because of excess amount of H_2O_2 , so it can be assumed H_2O_2 concentration is constant, thus the equation (4) can be changed to the following equations [33-35].

$$r = -\frac{d[\text{C}_{\text{DBT}}]}{dt} = k' [\text{C}_{\text{DBT}}] \quad (5)$$

$$-\frac{d[\text{C}_{\text{DBT}}]}{[\text{C}_{\text{DBT}}]^n} = k' dt \quad (6)$$

Equation (6) integration (with limit from initial concentration at time= 0 after bulk solution dark adsorption to concentration at time of irradiation) will lead to following equation:

$$\ln \frac{\text{C}_t}{\text{C}_0} = -k' t \quad (7)$$

Where C_0 is initial DBT concentration and C_t is final DBT concentrations [mol/l].

According to equation (7), the plotting of $\ln (\text{C}_0 / \text{C}_t)$ versus irradiation reaction time at different temperatures (40, 50, and 60°C) was shown in **Fig. 10**. The ODS reaction pseudo-first-order via high correlation factor (R2) for straight lines in **Fig. 10** and their slopes represented reaction rate constant as listed in the **Table 2**. As seen rate constants are increasing with temperature increasing because its power depends on temperature and it can be said that reaction followed pseudo-first-order reaction [35]; on the other hand, based on Arrhenius equation

$$[k = k_0 \exp(-E_a/RT)] \Leftrightarrow \ln k = \ln k_0 - \frac{E_a}{RT} \quad (8)$$

Where k_0 is pre exponential factor, R is universal gas constant (8.314 J / mol. K), T is absolute reaction temperate and E_a is reaction activation energy (J/mol). **Fig. 11** shows the relation between $\ln (k)$ versus $(1 / T)$, the activation energy is 26.8 kJ/mol under employed conditions for experiments.

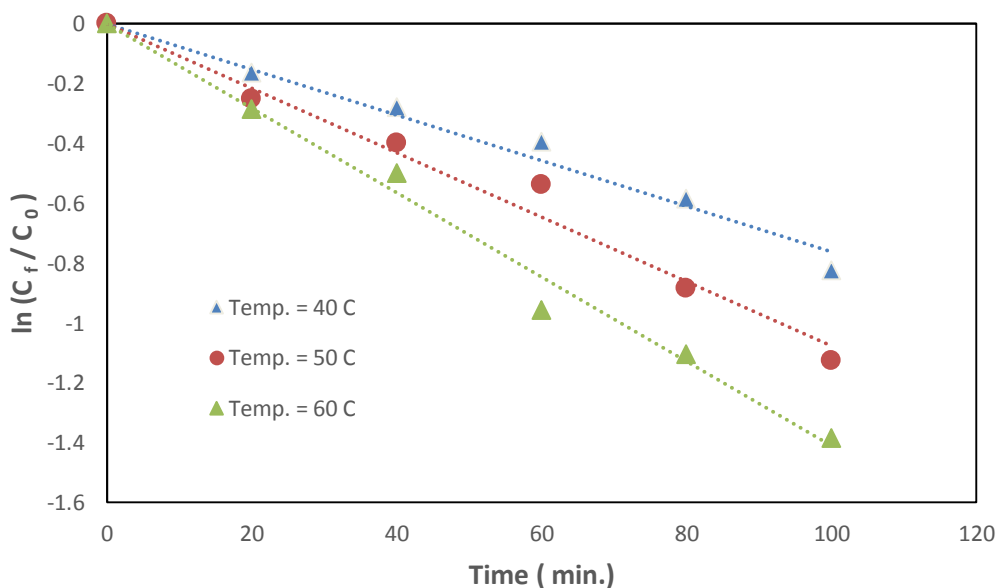


Fig.10: The model of reaction kinetics study by plotting of $\ln (\text{C}_0 / \text{C}_t)$ vs. time.

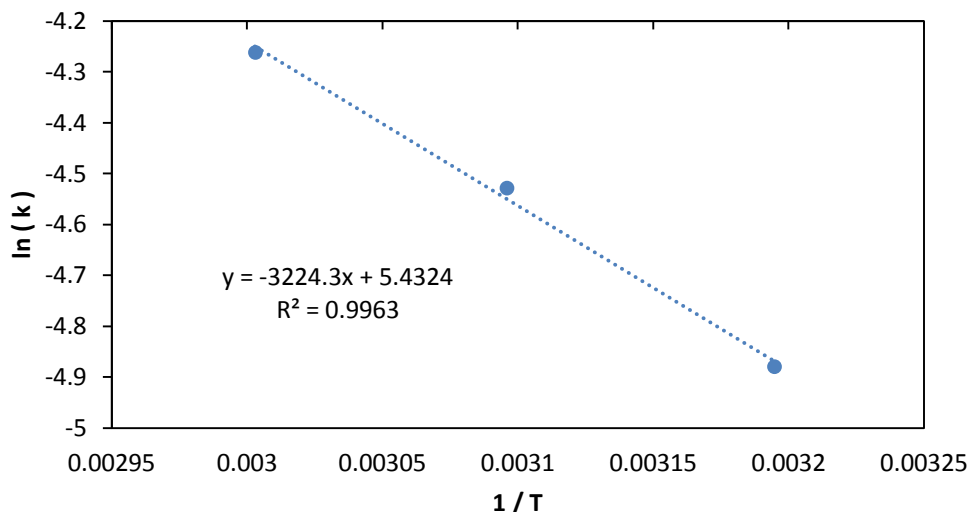


Fig.11: the effect of reaction temperature on reaction rate constant, Arrhenius activation energy for DBT oxidation.

Table 2: Reaction rate constant values with temperature and correlation factor R^2 .

Temperature (°C)	Reaction rate constant	R^2
40	0.0076	0.9666
50	0.0108	0.9804
60	0.0141	0.9874

Thermodynamics data for DBT oxidation photo catalytic reaction can be estimated as follows; the enthalpy change (ΔH) was calculated from activation energy [36]

$$\Delta H = E_a + RT \quad (9)$$

Then calculation of entropy change (ΔS) by:

$$\ln \left[\frac{k}{T} \right] = \ln \left(\frac{K_B}{h} \right) + \left(\frac{\Delta S}{R} \right) - \left(\frac{\Delta H}{RT} \right) \quad (10)$$

Where K_B and h are Boltzmann and Plank constants respectively. Thus plot of $\ln(k/T)$ against $(\Delta H/RT)$ can be established and the straight line was obtained and from line intercept entropy change was achieved as shown in **Fig. 12**. Finally the reaction Gibbs free energy (ΔG) value was estimated by

$$\Delta G = \Delta H - T\Delta S \quad (11)$$

The data obtained from the above were listed on **Table 3**, as seen, the DBT oxidation photo catalytic reaction

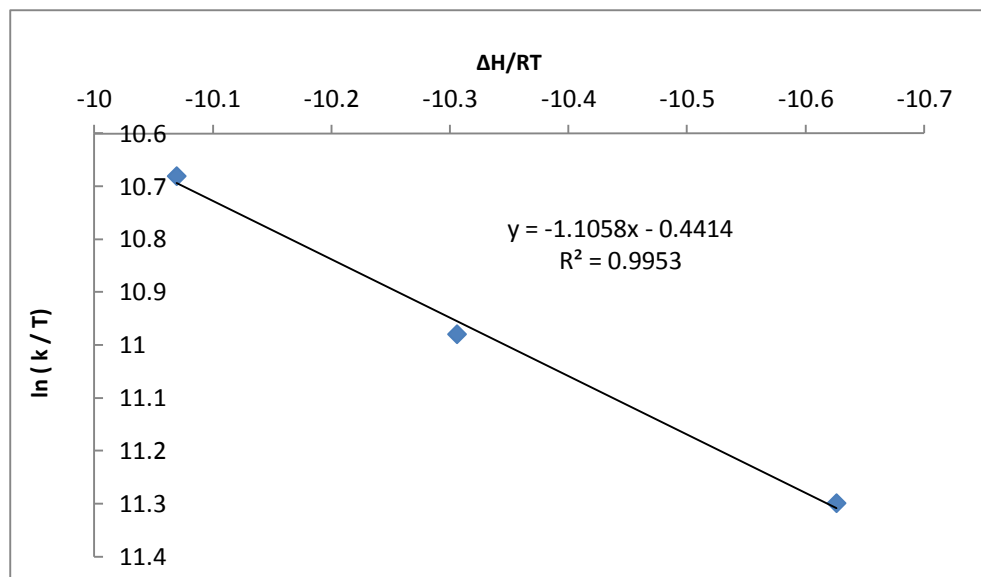


Fig.12: Typical plot used for the estimation of activation entropy for the reaction

Table 3: Kinetics and thermodynamic parameters for the photocatalytic DBT oxidation.

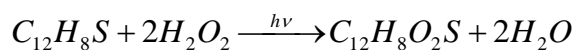
T (K)	k (min.)	Ea(kJ/mol)	ΔH(kJ/mol)	ΔS(kJ/mol)	ΔG(kJ/mol)
313	0.0076	26.8	29.402	-0.201	29.464
323	0.0108		29.485		29.549
333	0.0141		29.568		29.634

3.3. Proposed mechanism

The heterogeneous photocatalysis fundamentals are based on combination of semiconductors (metals oxides) with sulfides as photocatalyst under UV light, the electron was promoted from valence band VB to conduction band, and this electron e^-_{cb} was leaving hole h^+_{vb} , in case of charge separation is maintained, these electrons and holes may transfer to catalyst surface to participate redox reactions with absorbed compounds [12]. Conduction band CB electrons (e^-) and valence band VB holes (h^+) were generated when TiO_2 was irradiated with UV light, this electron will react with acceptor electron in H_2O_2 and this lead to hydroxyl radicals ($\bullet OH$) [16].



Active radicals which have ability to oxidize DBT to produce corresponding sulfones Dibenzothiophene -5,5 dioxide (DBTO₂).



The key of oxidative desulfurization reaction transfers sulfur organic components from oil phase (difficult to separate) to ionic liquid phase (easy to separate)[5], as shown in **Fig. 13**.

Scheme 1 shows the proposed mechanism for DBT oxidation over Cu oxides/TNT by photocatalytic technique; the mechanism based on the band gaps for TNT (3.2 eV), CuO (1.7 eV) and Cu₂O (2.1 eV) presents that the scheme is not scaled; it was used to explain the proposed mechanism. It was well known that TNT was characterized by a wide bandgap which made recombination between generated electrons and holes under visible light because excited electrons may not have enough energy to transfer to the conduction band, thus reaction will have suppressed but in the presence of copper oxides (Cu₂O and CuO which characterized by narrow bandgap), will promote to suppress recombination between electron and holes. Absorption radiation greater than TiO_2 bandgap energy level will generate electrons and holes at conduction and valence bands respectively so the generated electrons and holes are effectively separated under VL radiation, this excited electron at valence band at TNT conduction level through conduction band at Cu₂O. This excited electron is capable to interact with H_2O_2 at the TNT surface to produce hydroxyl radicals with a large amount and reaction of a photogenerated electron with H_2O_2 , the produced hydroxides radicals can oxidize BDT to produce its corresponding sulfones Dibenzothiophene, dioxide (DBTO₂). This mechanism suggests that TiO_2 plays as the main catalyst while CuO and Cu₂O act as co-catalyst which helps for charge separation promotion.

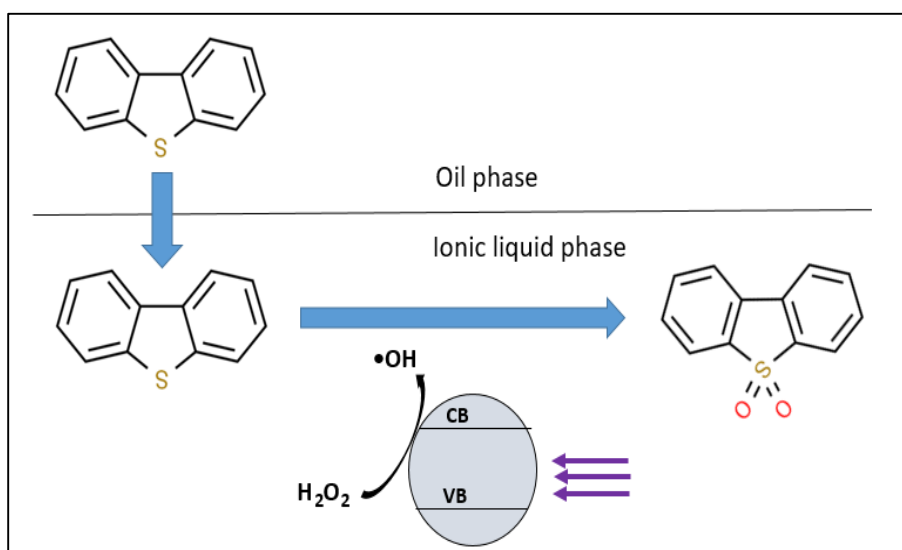
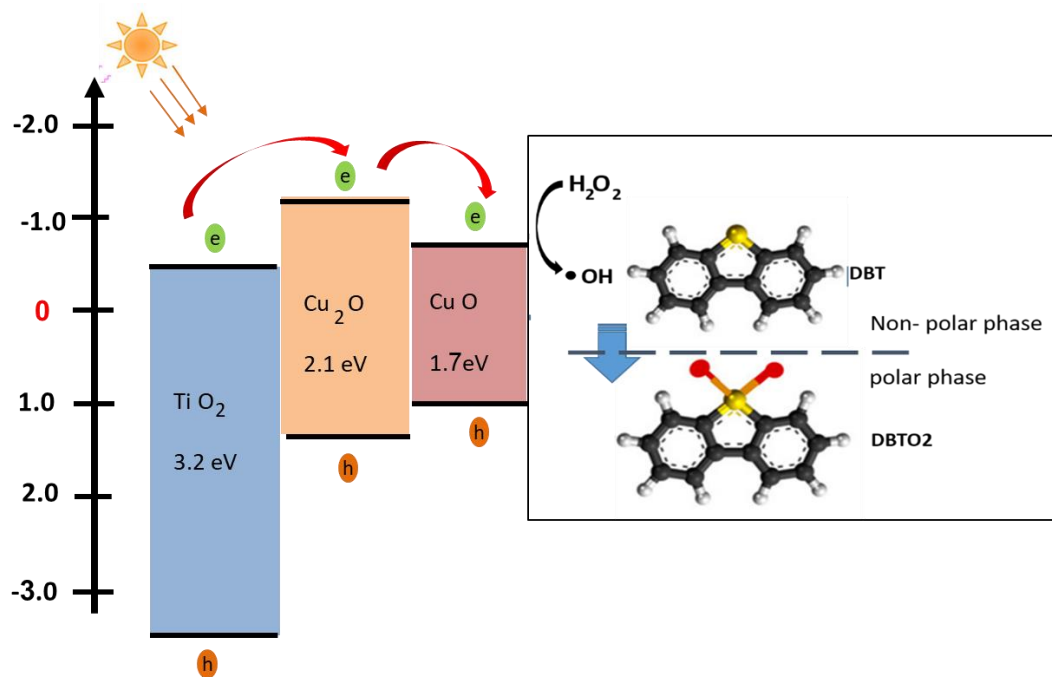


Fig. 13 :The suggested mechanism of photo catalytic desulfurization oxidative of Dibenzothiophene DBT[5].



Scheme 1: Proposed mechanism for DBT oxidation by H_2O_2 in presence of CuOx /TNT catalyst.

4. Conclusions

The increasing of TNT to VL sensitivity was done by modifying TNT with copper oxides to form CuOx /TNT catalyst, as shown in results for ODS reaction of DBT from fuel model. The expanded photocatalytic sensitivity of TNT was done by implanting it with copper oxides. According to the results, the sensitivity of TNT was expanded from UV irradiation to VL irradiation with high activity, in which the removal efficiency was 40.7 to 57.2 on TNT under VL irradiation and UV light irradiation and it was increased under VL irradiation by dipping TNT with copper oxides. Some operation variables on DBT oxidation photocatalytic reaction on implanted TNT with CuOx were studied; the results showed that DBT removal efficiency was increasing with reaction temperature, time, and oxidant amount (dosage) while it was decreased with increasing initial DBT concentration. Reaction kinetics studies show that ODS reaction for DBT oxidation follow pseud first-order reaction with the reaction rate constant of 0.076, 0.0108 and 0.0141 min^{-1} at 40,50 and 60 °C and with activation energy of 26.8 k J /mol obtained by Arrhenius equation. Thermodynamics calculations show that positive enthalpy change and Gibbs free energy change confirm a highly hydrate transition state complex, while negative entropy change -0.201 (near zero and relatively positive); this means that activated complex was not ordered than reactants which favor the rapid DBT oxidation.

Acknowledgements

The author would like to acknowledge Department of chemical engineering at university of Babylon for the support the work and also Mr. Riyadh Noman, the manager of chemical and petrochemical research center / Corporation of research and industry development / ministry of Industry and minerals and Mr. Quraish, Mr. Zuhair for their help in measuring sulfur content and finally Dr. Muhammed who is responsible on XRD, and all who helped to finish this work.

References

- [1] A. Fujishima, Tata N. Rao and Donald A. Tryk, Journal of Photochemistry and Photobiology C: Photochemistry Reviews, 1 (2000) 1-21.
- [2] Poulomi Roy, S. Berger and P. Schmuki, Angew.Chem.Int. Ed., 50 (2012) 2904-2939.
- [3] J. Liu and Pegah M. Hosseinpour, Journal of Vacuum Science and Technology A: Vacuum, Surface, and Films, 33 (2) (2015), p. 021202.
- [4] Qiu, X.; Miyauchi, M.; Sunada, K.; Minoshima, M.; Liu, M.; Lu, Y.; Li, D.; Shimodaira, Y.; Hosogi, Y.; Kuroda, Y. Acs Nano 6.2 (2012): 1609-1618.
- [5] H.-S. Kim, S.-K. Lee, and S.-H. Kang, Journal of the Korean Electrochemical Society, 15(3) (2012) 149-153,
- [6] J. B. Chen. C-Wei Wang, B-hong Ma, Yan Li, J. Wang, Rui -Sheng Guo and Wei-Min Liu, Thin Solid Films, 517(15), (2009) 4390-4393,
- [7] A.Nezamzadeh-Ejhi and M. Khorsandi, J. Hazard. Mater. 176, (2010) 629-637.

- [8] A. Nezamzadeh-Ejhih, Sh. Hushmandrad, *Appl. Catal. A: General*, 390 (2010) 110-118.
- [9] A. Pourtaheri, A. Nezamzadeh-Ejhih, *Spectrochimica Acta Part A: Molecular and Biomolecular Spectroscopy*, 137 (2015) 338-344.
- [10] H. H. Alwan, Ammar Ali Ali, and Hasan F. Makki. "Optimization of Oxidative Desulfurization Reaction with Fe₂O₃ Catalyst Supported on Graphene Using Box-Behnken Experimental Method." *Bulletin of Chemical Reaction Engineering & Catalysis*, 15.1 (2020): 175-185
- [11] H. H. Alwan, Hasan F. Makki and Tahssen A. Al-hattab, *Iran. J. Catal.*, 11(2), (2021) 101-111.
- [12] Y. Cui, Z. Ding, P. Liu, M. Antonietti, X. Fu, and X. Wang, *Physic. Chem. Chemical Physic.*, 14(4), (2012), 1455-1462,
- [13] X. Li, C. Chen, and J. Zhao, *Langmuir*, 17(13), (2001) 4118-4122.
- [14] Ling C., Tao J., Jindong Z., *Sci. Total Environ.* 776 (2021) 145840.
- [15] M. Keikhaei and M. Ichimura, *Int. J. Electrochem. Sci.*, 13(10), (2018) 9931-9941.
- [16] C. Wang, W. Zhu, Y. Xu, Hui Xu, M. Zhang, Y. Chao, S. Yin, H. Li, and L. Wang, *Ceramics International*, 40(8), (2014) 11627-11635.
- [17] Yasuda, Kouji, and Patrik Schmuki. *Electrochimica Acta* 52.12 (2007): 4053-4061.
- [18] D. Kim, F. Schmidt-Stein, R. Hahn, and P. Schmuki, *Electrochemistry Communications*, 10(7), (2008) 1082-1086.
- [19] S. Sreekantan, R. Hazan, and Z. Lockman, *Thin Solid Films*, 518(1), (2009) 16-21.
- [20] A. Ghicov, Sergiu P. Albu, R. Hahn, D. Kim, T. Stergiopoulos Dr., J. Kunze Dr., C. Albercht Schiller, p. Falaras Prof., P. Schmuki, *Chemistry-An Asian Journal*, 4 (4), 2009 520-525.
- [21] M. Balakrishnan and R. John, *Iran. J. Catal.* (2020) 10 (1) 1-16.
- [22] J. Ghijsen, L. H. Tjeng, J. van Elp, H. Eskes, J. Westerink, G. A. Sawatzky and M. Y. Czyzyk, *Physical Review B* 38.16 (1988): 11322.
- [23] Sarika P. Patil, Shital P. Patil, V. R. Puri and L. D. Jadhav, *AIP Conference Proceedings*, 1536 (2013) 1260-1261
- [24] Z. Amani-Beni, A. Nezamzadeh-Ejhih, *Journal of Colloid and Interface Science*, 504 (2017) 186-196.
- [25] Q. Ma, S. J. Liu, L. Q. Weng, Y. Liu, and B. Liu, *Journal of Alloys and Compounds*, 501 (2), (2010) 333-338.
- [26] X. Z. Li, F. B. Li, C. L. Yang, and W. K. Ge, *Journal of Photochemistry and Photobiology A: Chemistry*, 141 (2-3), (2001) 209-217.
- [27] J. Bandara, C. P. K. Udawatta, and C. S. K. Rajapakse, *Photochem. Photobiol. Sci.*, 4(11), (2005) 857-861.
- [28] Lan, X., C. Xu, G. Eang and H. Gao, *Catal. Today*, 140 (2009) 174-178.
- [29] G. Dedual, M. J. Macdonald, A. Alshareef, Z. Wu, D. C. W. Tsang, and A. C. K. Yip, *J. Environ. Chem. Eng.* 2 (4), (2014) 1947-1955.
- [30] Li, L., J. Zhang, C. Shen, Y. Wang, and G. Luo, *Fuel*, 167 (2016) 9-16.
- [31] A. Nezamzadeh-Ejhih, M. Karimi-Shamsabadi, *Chem. Eng. J.* 228 (2013) 631-641.
- [32] G. P. Zhu, W. S. Zhu, H. M. Li, W. L. Huang, Y. Q. Jiang, Y. X. Ding, and W. Jiang, *Petrol. Sci. Technol.*, 30 (2012), 2407-2416.
- [33] Angelo E. Choi, S. Roces, N. Dugos and M. Wan, *Fuel*, 180 (2016), 127-136.
- [34] M. Rezaei, A. Nezamzadeh-Ejhih, *Inter. J. Hydrogen Energy* 45 (2020) 24749-24764.
- [35] S. D. Khairnar, M. R. Patil, and V. S. Shrivastava, *Iran. J. Catal.*, 8 (2), 2018, 143-150.
- [36] Gupta, Nirja, Ajai Kumar Pillai, and Prachi Parmar, *Spectrochimica Acta Part A: Molecular and Biomolecular Spectroscopy*, 139 (2015): 471-476.